

Three-body photodisintegration of ${}^3\text{He}^\dagger$

B. F. Gibson

*Theoretical Division, Los Alamos Scientific Laboratory,
University of California, Los Alamos, New Mexico 87545*

D. R. Lehman

Department of Physics, The George Washington University, Washington, D. C. 20052

(Received 29 September 1975)

Cross sections for three-body photodisintegration of ${}^3\text{He}$ are calculated in the electric dipole approximation. The calculation is performed within the context of exact three-body theory with the two-nucleon interactions represented by s -wave spin-dependent separable potentials fitted to low-energy nucleon-nucleon scattering data. The photodisintegration amplitude is expressed in terms of the fully off-shell nucleon-plus-correlated-pair amplitudes, a method applicable to any weak-process disintegration amplitude. The numerical results indicate: (1) The ${}^3\text{He}(\gamma, n)2p$ total cross section has a peak value of approximately 1 mb. (2) The neutron spectra for ${}^3\text{He}(\gamma, n)2p$ and the proton spectra for ${}^3\text{He}(\gamma, p)n$ peak sharply in the region of the strong p - p final-state interaction.

[NUCLEAR REACTIONS Photodisintegration of ${}^3\text{He}$; exact three-body calculation; separable potentials; neutron and proton spectra.]

I. INTRODUCTION

The trinucleon system provides an excellent test of our understanding of nuclear physics beyond the simple two-body problem. This three-body problem is sufficiently complex that it tests the details of the underlying two-nucleon input. Yet, the calculations are in principle exact, so that one is not forced to approximate the solution prematurely. The photodisintegration of ${}^3\text{H}$ and ${}^3\text{He}$ is especially useful in realistic trinucleon studies since the ground state is reasonably well understood, the interaction operator is known, and the resulting continuum is dominated by a single partial wave ($l=1$). We have previously considered the two-body photodisintegration reaction leading to the d - N final state.¹ Here we report our formulation of the three-body photodisintegration reaction and compare numerical results with the available data.²⁻⁵

The previous calculation of this type was done by Barbour and Phillips.⁶ They showed that the rescattering effects in a correct treatment of the final state were all important in understanding the physics involved. The $T = \frac{1}{2}$ three-body channel was strongly suppressed—most of that isospin strength appearing instead in the two-body channel. The $T = \frac{3}{2}$ three-body channel (there is no $T = \frac{3}{2}$ two-body channel) showed large rescattering effects as the cross section peak was moved from the 20–25 MeV photon energy region to below 15 MeV. Although the shape of the spectrum was

found to be in reasonable agreement with the data,^{2,3} the magnitude of the cross section exceeded the data in the region of the peak by some 20%. Recently, Fabre and Levinger have published a calculation of the $T = \frac{3}{2}$ component of the cross section using the lowest hyperspherical harmonic.⁷ Their calculation does not show the strong enhancement of the cross section below photon energies of 20 MeV that was present in the results of Ref. 6. In addition to the data of Refs. 2 and 3 considered by Barbour and Phillips, there now exist the data of Berman, Fultz, and Yergin⁴ and the recently completed analysis of Gorbunov.⁵ These new data tend to confirm that the normalization of the calculation reported in Ref. 6 is somewhat high.

In this investigation, we have reformulated the theory so that the photodisintegration amplitude is given by an integral involving the N - d and N - ϕ off-shell scattering amplitudes. It is these off-shell scattering amplitudes, instead of the photodisintegration amplitudes, that are determined by a set of coupled integral equations. In addition to permitting us to calculate separately the two-body and three-body photodisintegration amplitudes, this formulation of the problem provides a natural extension to other similar reactions such as electrodisintegration, pion absorption, etc.

We carry out this investigation using the mathematically simplifying separable potential representation of the N - N interaction, as did Barbour and Phillips. The parameters of the s -wave spin-

dependent rank-one potentials are determined from the N - N singlet and triplet effective-range parameters. Unlike Barbour and Phillips, we use these potentials to determine the initial as well as the final state. We would prefer to compare with the ^3H reaction, where there are no Coulomb problems; however, because the available data are for the ^3He reaction, we restrict our numerical consideration to that nucleus. As in Ref. 6, we neglect the pure Coulomb p - p interaction in the final state; however, we do remark on inclusion of the Coulomb effect in the strong interaction.

Our three-body formalism is described in detail in Sec. II. We apply it to the ^3He photodisintegration reaction in Sec. III. The numerical results and comparison with the data are presented in Sec. IV. Section V summarizes our conclusions.

II. FORMALISM FOR THREE-BODY BREAKUP

In parallel to our presentation of the two-body breakup formalism in Sec. II of Ref. 1, we develop in this section the corresponding theory for three-body breakup of a three-body nucleus. The interaction which is responsible for the disintegration process is assumed to be such that it can be treated perturbatively.

Consider the three-body total Hamiltonian

$$H_{\text{total}} = H + H', \quad (1)$$

where

$$H = H_0 + V \quad (2)$$

and

$$V = \sum_{\alpha=1}^3 V_{\alpha} = \sum_{i<j}^3 V_{ij}. \quad (3)$$

The H' represents that part of the interaction which is to be treated perturbatively, H_0 is the kinetic-energy operator, and V_{ij} is the nuclear-interaction operator for particles i and j . Specifically, H is assumed to have a spectrum including at least a three-body bound state and a scattering state of three unbound particles, but it could also have a scattering state of a particle plus bound pair provided one of the nuclear potentials can support a two-body bound state. For the two former states, respectively, we have

$$H|\Psi_B\rangle = -E_B|\Psi_B\rangle, \quad E_B > 0, \quad (4)$$

$$H|\Psi_{\alpha n \vec{p} \vec{k}}\rangle = E_{\alpha n}^{(3)}|\Psi_{\alpha n \vec{p} \vec{k}}\rangle, \quad E_{\alpha n}^{(3)} = \frac{\vec{p}_{\alpha}^2}{2m_{\alpha}} + \frac{k_{\beta\gamma}^2}{2\mu_{\beta\gamma}}, \quad (5)$$

where \vec{p}_{α} is the relative momentum of particle α with respect to the center of mass of particles β and γ , $\vec{k}_{\beta\gamma}$ is the relative momentum of particles β and γ , the reduced masses m_{α} and $\mu_{\beta\gamma}$ are ex-

pressed in terms of the particle masses, designated M_{α} , as

$$m_{\alpha} = \frac{M_{\alpha}(M_{\beta} + M_{\gamma})}{M_{\alpha} + M_{\beta} + M_{\gamma}}, \quad (6)$$

$$\mu_{\beta\gamma} = \frac{M_{\beta}M_{\gamma}}{M_{\beta} + M_{\gamma}} \quad (7)$$

with $\alpha \neq \beta \neq \gamma \neq \alpha$ and each index permitted to have the values 1 to 3.

In this paper, we are concerned with three-body disintegration amplitudes

$$A_3(\alpha, n, \vec{p}, \vec{k}) = \langle \Psi_{\alpha n \vec{p} \vec{k}}^{(-)} | H' | \Psi_B \rangle, \quad (8)$$

where the superscript $(-)$ denotes the outgoing state which asymptotically corresponds to an incoming wave. The three-body scattering state is a solution of

$$|\Psi_{\alpha n \vec{p} \vec{k}}^{(-)}\rangle = [1 - G(E_{\alpha n}^{(3)} - i\eta)V]|\Phi_{\alpha n \vec{p} \vec{k}}^0\rangle \quad (9)$$

with $\eta > 0$,

$$H_0|\Phi_{\alpha n \vec{p} \vec{k}}^0\rangle = E_{\alpha n \vec{p} \vec{k}}^{(3)}|\Phi_{\alpha n \vec{p} \vec{k}}^0\rangle, \quad (10)$$

and the resolvent operator is defined as

$$G(z) = (H - z)^{-1}. \quad (11)$$

We define the operator

$$\Omega_0^{(+)}(z) = \Omega_0(z + i\eta) = 1 - VG(z + i\eta) \quad (12)$$

and write the three-body disintegration amplitude as

$$A_3(\alpha, n, \vec{p}, \vec{k}) = \langle \Phi_{\alpha n \vec{p} \vec{k}}^0 | \Omega_0^{(+)}(z) H' | \Phi_B \rangle. \quad (13)$$

The crux of our development lies in the fact that $\Omega_0^{(+)}(z)$ can be expressed in terms of the transition operator $X_{0\alpha}(z)$ which connects a particle-plus-correlated-pair state with a state of three uncorrelated particles. This can be demonstrated by formal operator manipulations or by the iterative method used in Ref. 1. Specifically, we derive

$$\Omega_0^{(+)}(z) = 1 - \sum_{\beta=1}^3 T_{\beta}(z) G_0(z) \Omega_{\beta}^{(+)}(z) \quad (14)$$

$$= 1 - \sum_{\beta=1}^3 G_0^{-1}(z) X_{0\beta}(z) T_{\beta}(z) G_0(z), \quad (15)$$

where $T_{\beta}(z)$ is the two-body T operator defined as

$$T_{\beta}(z) G_0(z) = V_{\beta} G_{\beta}(z), \quad (16)$$

$$G_0(z) = (H_0 - z)^{-1}, \quad (17)$$

$$G_{\beta}(z) = (H_0 + V_{\beta} - z)^{-1}, \quad (18)$$

the operator $\Omega_{\alpha}^{(+)}(z)$ satisfies

$$\Omega_{\alpha}^{(+)}(z) = 1 - \sum_{\beta=1}^3 (1 - \delta_{\alpha\beta}) T_{\beta}(z) G_0(z) \Omega_{\beta}^{(+)}(z) \quad (19)$$

and

$$X_{0\beta}(z) = G_0(z) - G_0(z) \sum_{\gamma=1}^3 T_\gamma(z) X_{\gamma\beta}(z). \quad (20)$$

The three-particle dynamics of the continuum state now reside in the transition operators, $X_{\gamma\beta}(z)$ which connect particle-plus-correlated-pair states and are solutions of the operator equations

$$X_{\alpha\beta}(z) = G_0(z)(1 - \delta_{\alpha\beta}) - \sum_{\gamma} X_{\alpha\gamma}(z) T_\gamma(z) (1 - \delta_{\gamma\beta}) G_0(z) \quad (21)$$

or

$$X_{\alpha\beta}(z) = G_0(z)(1 - \delta_{\alpha\beta}) - G_0(z) \sum_{\gamma} (1 - \delta_{\alpha\gamma}) T_\gamma(z) X_{\gamma\beta}(z). \quad (22)$$

The three-body disintegration amplitude is then written as the sum of three terms:

$$A_3(\alpha, n, \vec{p}, \vec{k}) = \langle \Phi_{\alpha n \vec{p} \vec{k}}^0 | H' | \Psi_B \rangle - \sum_{\beta=1}^3 \langle \Phi_{\alpha n \vec{p} \vec{k}}^0 | T_\beta(z) G_0(z) H' | \Psi_B \rangle + \sum_{\beta, \gamma=1}^3 \langle \Phi_{\alpha n \vec{p} \vec{k}}^0 | T_\gamma(z) X_{\gamma\beta}(z) T_\beta(z) G_0(z) H' | \Psi_B \rangle \quad (23)$$

with $z = E_{\alpha n}^{(3)} + i\eta$. The three terms in Eq. (22) are designated the plane-wave Born term, first-rescattering term, and the term which sums all rescatterings beyond the first, respectively.⁸

In Ref. 1 the usefulness of expressing the two-body disintegration amplitude in terms of the particle-plus-correlated-pair amplitude was made apparent. The final-state three-particle dynamics are separated from the disintegration of the ground state due to H' . As can be seen from Eq. (23) and from our application of Eq. (23) to three-body photodisintegration of ${}^3\text{He}$ in Sec. III, this is also the case for three-body disintegration processes. Once the particle-plus-correlated-pair amplitudes are generated from given phenomenological two-particle interactions, two- or three-body disintegration processes reduce to calculating the effect of H' on $|\Psi_B\rangle$ and folding the result with either a plane-wave state or a particle-plus-correlated-pair state. As mentioned in the Introduction, the point is that, for a given set of two-particle interactions and a specified three-particle excitation energy, the three-particle continuum amplitudes need be calculated only once to compute the amplitudes for several different disintegration mechanisms.

III. APPLICATION OF FORMALISM TO THREE-BODY PHOTODISINTEGRATION OF ${}^3\text{He}$

We now apply our formalism of the previous section to three-body photodisintegration of ${}^3\text{He}$ assuming separable nuclear interactions. The two-nucleon transition operator in the three-particle Hilbert space is taken to be attractive, s -wave, spin-dependent, but charge-independent:

$$T_\alpha(z) = - \sum_{n=s}^t |g_{\alpha n}\rangle \tau_{\alpha n}(z) \langle g_{\alpha n}| (|SI\rangle \langle SI|)_{\alpha n}, \quad (24)$$

where

$$\tau_{\alpha n}(z) = \frac{\lambda_n}{2\mu_\alpha} \left(1 - \frac{\lambda_n}{2\mu_\alpha} \langle g_{\alpha n} | G_0(z) | g_{\alpha n} \rangle \right)^{-1}. \quad (25)$$

The lower-case letters s and t denote singlet and triplet spin, respectively, for the interacting nucleon pair, while the upper-case letter S (I) represents the total spin (isospin) of the three-nucleon system obtained by coupling the spin (isospin) of the noninteracting particle α to the spin (isospin) of the interacting pair $\beta\gamma$. The strength of the interaction is given by λ_n and the form factors $|g_{\alpha n}\rangle$ determine its range.

Prior to specifying the form of H' for this problem, a considerable amount of algebra can be carried through for Eq. (23) solely on the basis of the interaction defined by Eq. (24) and the assumption of identical nucleons each with mass M . The plane-wave Born term in Eq. (23) does not require knowledge of $T_\alpha(z)$, so we ignore it for the moment and consider the first-rescattering term and then the term which sums all rescatterings beyond the first.

The first-rescattering term is rewritten by first inserting $T_\beta(z)$:

$$\begin{aligned} & \langle \Phi_{\alpha n \vec{p} \vec{k}}^0 | T_\beta(z) G_0(z) H' | \Psi_B \rangle \\ &= - \sum_{m=s}^t \langle \Phi_{\alpha n \vec{p} \vec{k}}^0 | g_{\beta m} \rangle \tau_{\beta m}(z) \langle g_{\beta m} | G_0(z) H' | \Psi_B \rangle, \quad (26) \end{aligned}$$

$$\begin{aligned} & \langle \Phi_{\alpha n \vec{p} \vec{k}}^0 | T_\beta(z) G_0(z) H' | \Psi_B \rangle \\ &= - \sum_{m=s}^t \langle \vec{k}_\beta n | g_{\beta m} \rangle \tau_{\beta m} \left(z - \frac{3\vec{p}_\beta^2}{4M} \right) \\ & \quad \times \langle g_{\beta m} \vec{p}_\beta | G_0(z) H' | \Psi_B \rangle, \quad (27) \end{aligned}$$

where $\langle \vec{p}_\alpha \vec{k}_\alpha | = \langle \vec{p}_\beta \vec{k}_\beta | = \langle \vec{p}_\gamma \vec{k}_\gamma |$ has been used and the total spin-isospin projection has been suppressed. The unsymmetrized first-rescattering term is obtained from Eq. (27) by multiplying with (-1) and summing over β . The symmetrized form of the first-rescattering term is generated by summing over α and dividing by $\sqrt{3}$. This procedure yields, after some manipulation,

$$\begin{aligned}
& -\left(\frac{1}{3}\right)^{1/2} \sum_{\alpha=1}^3 \sum_{\beta=1}^3 \langle \Phi_{\alpha n \vec{k}}^0 | T_{\beta}(z) G_0(z) H' | \Psi_B \rangle \\
& = \sum_{m=s}^t \sum_{\alpha=1}^3 \langle \vec{k}_{\alpha} n | g_{\alpha m} \rangle \tau_m \left(z - \frac{3p_{\alpha}^2}{4M} \right) B_m^0(z, \vec{p}_{\alpha}), \quad (28)
\end{aligned}$$

where $\tau_m \equiv \tau_{m\alpha}$, since the subscript α would now be redundant and

$$B_n^0(z, \vec{p}_{\beta}) = \left(\frac{1}{3}\right)^{1/2} \sum_{\alpha} \langle g_{\alpha n} \vec{p}_{\alpha} | G_0(z) H' | \Psi_B \rangle. \quad (29)$$

$B_n^0(z, \vec{p}_{\beta})$ is the off-shell Born amplitude.

The third term in Eq. (23) is handled in a similar manner. Firstly, we insert the explicit form of the two-body transition operators. This step yields

$$\langle \Phi_{\alpha n \vec{k}}^0 | T_{\gamma}(z) X_{\gamma\beta}(z) T_{\beta}(z) G_0(z) H' | \Psi_B \rangle = \sum_{m=s}^t \sum_{m'=s}^t \langle \Phi_{\alpha n \vec{k}}^0 | g_{\gamma m} \rangle \tau_{\gamma m}(z) \langle g_{\gamma m} | X_{\gamma\beta}(z) | g_{\beta m'} \rangle \tau_{\beta m'}(z) \langle g_{\beta m'} | G_0(z) H' | \Psi_B \rangle \quad (30)$$

or

$$\begin{aligned}
\langle \Phi_{\alpha n \vec{k}}^0 | T_{\gamma}(z) X_{\gamma\beta}(z) T_{\beta}(z) G_0(z) H' | \Psi_B \rangle & = \sum_{m=s}^t \sum_{m'=s}^t \langle \vec{k}_{\gamma} n | g_{\gamma m} \rangle \tau_{\gamma m} \left(z - \frac{3p_{\gamma}^2}{4M} \right) \int d^3 p_{\beta} \langle g_{\gamma m} \vec{p}_{\gamma} | X_{\gamma\beta}(z) | g_{\beta m'} \vec{p}_{\beta} \rangle \tau_{\beta m'} \left(z - \frac{3p_{\beta}^2}{4M} \right) \\
& \quad \times \langle g_{\beta m'} \vec{p}_{\beta} | G_0(z) H' | \Psi_B \rangle, \quad (31)
\end{aligned}$$

where, again, the total spin-isospin projection has been suppressed and use made of the fact that $\langle \vec{p}_{\alpha} \vec{k}_{\alpha} | = \langle \vec{p}_{\gamma} \vec{k}_{\gamma} |$. Secondly, the contribution of this term to the unsymmetrized amplitude is obtained by summing Eq. (31) over β and γ . Finally, the symmetrized contribution follows from the latter result by summing over α and dividing by $\sqrt{3}$. After some algebra, we derive

$$\begin{aligned}
& \left(\frac{1}{3}\right)^{1/2} \sum_{\alpha=1}^3 \sum_{\beta=1}^3 \sum_{\gamma=1}^3 \langle \Phi_{\alpha n \vec{k}}^0 | T_{\gamma}(z) X_{\gamma\beta}(z) T_{\beta}(z) G_0(z) H' | \Psi_B \rangle \\
& = \sum_{\alpha=1}^3 \sum_{m=s}^t \sum_{m'=s}^t \langle \vec{k}_{\alpha} n | g_{\alpha m} \rangle \tau_m \left(z - \frac{3p_{\alpha}^2}{4M} \right) \int d^3 p' \langle \vec{p}_{\alpha} | X_{mm'}(z) | \vec{p}' \rangle \tau_{m'} \left(z - \frac{3p'^2}{4M} \right) B_{m'}^0(z, \vec{p}'), \quad (32)
\end{aligned}$$

where

$$\langle \vec{p} | X_{mm'}(z) | \vec{p}' \rangle = \frac{1}{3} \sum_{\alpha=1}^3 \sum_{\beta=1}^3 \langle g_{\alpha m} \vec{p} | X_{\alpha\beta}(z) | g_{\beta m'} \vec{p}' \rangle. \quad (33)$$

The full symmetrized three-body disintegration amplitude is obtained from Eq. (22) by summing over α and dividing by $\sqrt{3}$. This procedure leads to

$$M_3^n(z, \vec{p}, \vec{k}) = \left(\frac{1}{3}\right)^{1/2} \sum_{\alpha=1}^3 A_3(\alpha, n, \vec{p}, \vec{k}) \quad (34)$$

or

$$\begin{aligned}
M_3^n(z, \vec{p}, \vec{k}) & = C_0^n(\vec{p}, \vec{k}) + \sum_{m=s}^t \sum_{\alpha=1}^3 \langle \vec{k}_{\alpha} n | g_{\alpha m} \rangle \tau_m \left(z - \frac{3p_{\alpha}^2}{4M} \right) B_m^0(z, \vec{p}_{\alpha}) \\
& \quad + \sum_{\alpha=1}^3 \sum_{m=s}^t \sum_{m'=s}^t \langle \vec{k}_{\alpha} n | g_{\alpha m} \rangle \tau_m \left(z - \frac{3p_{\alpha}^2}{4M} \right) \int d^3 p' \langle \vec{p}_{\alpha} | X_{mm'}(z) | \vec{p}' \rangle \tau_{m'} \left(z - \frac{3p'^2}{4M} \right) B_{m'}^0(z, \vec{p}') \quad (35)
\end{aligned}$$

with

$$z = \frac{3p^2}{4M} + \frac{k^2}{M} + i\eta, \quad C_0^n(\vec{p}, \vec{k}) = \left(\frac{1}{3}\right)^{1/2} \sum_{\alpha=1}^3 \langle \Phi_{\alpha n \vec{k}}^0 | H' | \Psi_B \rangle, \quad (36)$$

where use has been made of Eqs. (29) and (33). The fully-off-shell three-particle scattering amplitude under the integral in Eq. (35) satisfies the integral equation

$$\langle \vec{p} | X_{nn'}(z) | \vec{p}' \rangle = \langle \vec{p} | Z_{nn'}(z) | \vec{p}' \rangle + \sum_{m=s}^t \int d^3 p'' \langle \vec{p} | X_{nm}(z) | \vec{p}'' \rangle \tau_m \left(z - \frac{3p''^2}{4M} \right) \langle \vec{p}'' | Z_{m'n'}(z) | \vec{p}' \rangle, \quad (37)$$

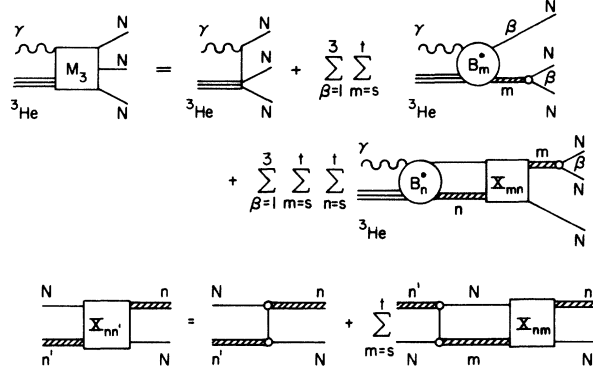


FIG. 1. Diagrammatic representation of the calculation of the three-body photodisintegration amplitude. The wavy line represents the disintegration mechanism (i.e., in the case of photodisintegration a photon), the triple lines the trinucleon ground state, and the cross-hatched double lines a particular correlated pair plus nucleon (N) being off shell. The upper part of the figure describes the amplitude M_3 as a sum of Born, first-rescattering, and integral over the off-shell scattering amplitude X_{mn} ; B_m^0 is the off-shell Born amplitude. The lower part of the figure describes the integral equation that determines the off-shell scattering amplitude $X_{nn'}$.

where

$$\langle \vec{p} | Z_{nn'}(z) | \vec{p}' \rangle = \frac{1}{3} \sum_{\alpha=1}^3 \sum_{\beta=1}^3 (1 - \delta_{\alpha\beta}) \langle g_{\alpha n} \vec{p} | G_0(z) | g_{\beta n'} \vec{p}' \rangle. \quad (38)$$

The last two equations follow from Eqs. (20) and (33). Equations (35) and (37) are readily interpreted in terms of a diagrammatic representation as in Fig. 1 and explained in the accompanying caption. To apply Eq. (34) to ${}^3\text{He}$ photodisintegration, we must specify H' and $|\Psi_B\rangle$, plus classify the set of spin-isospin projections $\{n\}$.

As implied in the Introduction, ${}^3\text{He}$ photodisintegration is primarily an electric dipole transition. Therefore, we write the perturbative Hamiltonian as

$$H' = \frac{1}{2} e \sum_{i=1}^3 (\hat{\epsilon} \cdot \vec{r}_i) \tau_3^{(i)}, \quad (39)$$

where the \vec{r}_i are the nucleon center-of-mass coordinates, $\hat{\epsilon}$ is the photon polarization unit vector, e is the electric charge, and $\tau_3^{(i)}$ is the third (z component) isospin Pauli matrix for particle i . H' operates on the ground state $|\Psi_B\rangle$ which, for ${}^3\text{He}$, we take to be only the dominant spatially symmetric component. The result of operating with H' on

$$|\Psi_B\rangle = \psi_0^s \xi^a \quad (40)$$

TABLE I. Amplitude projections.

Total isospin	Spatial symmetry for particles 2 and 3		Spin-isospin function	
	S_{23}	I_{23}	S_{23}	I_{23}
$\frac{1}{2}$	s	0	1	$\chi' \eta''$
	a	0	0	$\chi' \eta'$
	s	1	0	$\chi'' \eta'$
	a	1	1	$\chi'' \eta''$
$\frac{3}{2}$	s	0	1	$\chi' \eta^s$
	a	1	1	$\chi'' \eta^s$

is

$$H' |\Psi_B\rangle = \left(\frac{-e}{2\sqrt{3}} \right) \hat{\epsilon} \cdot \left[\frac{2}{\sqrt{3}} \vec{p} \xi' - \vec{r} \xi'' - \left(\frac{2}{\sqrt{3}} \vec{p} \chi' - \vec{r} \chi'' \right) \eta^s \right] \psi_0^s. \quad (41)$$

In Eq. (41), \vec{p} and \vec{r} are the standard Jacobi variables for three identical particles conjugate to \vec{p} and \vec{k} used above, e.g.,

$$\vec{p} = \vec{r}_1 - \frac{1}{2}(\vec{r}_2 + \vec{r}_3) = \frac{3}{2}\vec{r}_1, \quad (42a)$$

$$\vec{r} = \vec{r}_2 - \vec{r}_3, \quad (42b)$$

and $\chi'(1, 23)$ [$\chi''(1, \overline{23})$] is a spin- $\frac{1}{2}$ function obtained by first coupling the spins of nucleons 2 and 3 to spin zero [one]; the spin-isospin functions are

$$\xi^a = \frac{1}{\sqrt{2}} (\chi' \eta'' - \chi'' \eta'), \quad (43a)$$

$$\xi' = \frac{1}{\sqrt{2}} (\chi' \eta'' + \chi'' \eta'), \quad (43b)$$

$$\xi'' = \frac{1}{\sqrt{2}} (\chi' \eta' - \chi'' \eta'') \quad (43c)$$

with the isospin function η' and η'' defined analogously to χ' and χ'' , respectively, and η^s is the isospin- $\frac{3}{2}$ function for three nucleons. Equation (41) is the basis for working out the details of the terms in Eq. (35), but first we must discuss the set of spin-isospin projections.

We classify the spin-isospin projections $\{n\}$ according to total isospin I , the spin and isospin couplings between particles 2 and 3 (S_{23} and I_{23} , respectively), and the spatial symmetry of particles 2 and 3. The final state can have only total spin $\frac{1}{2}$ since the ground state is total spin $\frac{1}{2}$ and the transition operator is spin-independent. If the spatial-spin-isospin projection function is constructed to be antisymmetric under interchange of particles 2 and 3, we can operate with it directly in Eq. (35) to obtain the appropriate amplitude because Eq. (35) has been symmetrized. The six possible spatial-spin-isospin projections are given in Table I. It is now clear that the three quantum numbers I ,

S_{23} , and I_{23} are sufficient to specify the various amplitude projections, i.e., $M_3^n(z, \vec{p}, \vec{k}) \equiv M_{S_{23}I_{23}}^I(z, \vec{p}, \vec{k})$.

We begin explicitly constructing the six possible amplitudes for three-body ${}^3\text{He}$ photodisintegration by considering the plane-wave Born term $C_0^n(\vec{p}, \vec{k})$ Eq. (36). Projecting with the spin-isospin functions listed in Table I on $H'|\Psi_B\rangle$ as given in Eq. (41), and multiplying by $\sqrt{3}$ to account for $\sqrt{\frac{1}{3}}$ times the sum over α in Eq. (36), we obtain [notation $C_0^n(\vec{p}, \vec{k}) \equiv C_{S_{23}I_{23}}^I(\vec{p}, \vec{k})$]

$$C_{01}^{1/2}(\vec{p}, \vec{k}) = -e\sqrt{\frac{1}{6}} \hat{\epsilon} \cdot \vec{p}_{op} \psi_0^s(\vec{k}, \vec{p}), \quad (44a)$$

$$C_{00}^{1/2} = e\frac{1}{2\sqrt{3}} \hat{\epsilon} \cdot \vec{r}_{op} \psi_0^s, \quad (44b)$$

$$C_{10}^{1/2} = C_{01}^{1/2}, \quad (44c)$$

$$C_{11}^{1/2} = -C_{00}^{1/2}, \quad (44d)$$

$$C_{01}^{3/2} = -\sqrt{2}C_{01}^{1/2}, \quad (44e)$$

$$C_{11}^{3/2} = \sqrt{2}C_{11}^{1/2}, \quad (44f)$$

where $\vec{p}_{op} = -i\hbar\vec{\nabla}_p$ and $\vec{r}_{op} = -i\hbar\vec{\nabla}_k$. Next, the same is done for the first-rescattering term, designated $F_{S_{23}I_{23}}^I(z, \vec{p}, \vec{k})$, remembering that in the expression in Eq. (35) the spin-isospin projections for the interactions are suppressed. Since the two-nucleon interactions are taken to be s wave only, it is sufficient to denote $B_m^n(z, \vec{p})$ by simply adding a superscript for total isospin— $B_m^{0I}(z, \vec{p})$. Explicitly, we derive

$$F_{01}^{1/2}(z, \vec{p}, \vec{k}) = \frac{1}{2}\{T^s[f_s^{1/2}(1) - f_t^{1/2}(1)] - T''[f_s^{1/2}(1) + f_t^{1/2}(1)]\}, \quad (45a)$$

$$F_{00}^{1/2} = \frac{1}{2}T'[f_s^{1/2}(1) + f_t^{1/2}(1)], \quad (45b)$$

$$F_{10}^{1/2} = -\frac{1}{2}\{T^s[f_s^{1/2}(1) - f_t^{1/2}(1)] + T''[f_s^{1/2}(1) + f_t^{1/2}(1)]\}, \quad (45c)$$

$$F_{11}^{1/2} = -F_{00}^{1/2}, \quad (45d)$$

$$F_{01}^{3/2} = -T''f_s^{3/2}(1), \quad (45e)$$

$$F_{11}^{3/2} = T'f_s^{3/2}(1), \quad (45f)$$

where the permutation operators are defined as

$$T^s = (23) + (31) + (12), \quad (46a)$$

$$T'' = -(23) + \frac{1}{2}[(12) + (31)], \quad (46b)$$

$$T' = \frac{1}{2}\sqrt{3}[(31) - (12)], \quad (46c)$$

and

$$f_n^I(\alpha) = g_n(\vec{k}_\alpha) \tau_n \left(z - \frac{3p_\alpha^2}{4M} \right) B_n^{0I}(z, \vec{p}_\alpha) \quad (47)$$

with $\langle \vec{k}_\alpha | g_n \rangle \equiv g_n(\vec{k}_\alpha)$. The explicit forms for the off-shell Born amplitudes are ($n = s$ or t)

$$B_n^{01/2}(z, \vec{p}) = -\frac{eM}{\sqrt{6}} \int d^3k \frac{g_n(k) [\hat{\epsilon} \cdot \vec{p}_{op} \psi_0^s(\vec{k}, \vec{p})]}{3p^2/4 + k^2 - Mz} \quad (48)$$

and

$$B_s^{03/2}(z, \vec{p}) = -\sqrt{2}B_s^{01/2}(z, \vec{p}). \quad (49)$$

Finally, the third term in Eq. (35) designated $S_{S_{23}I_{23}}^I(z, \vec{p}, \vec{k})$ yields by means of similar algebraic manipulations the following:

$$S_{01}^{1/2}(z, \vec{p}, \vec{k}) = \frac{1}{2}\{T^s[S_s^{1/2}(1) - S_t^{1/2}(1)] - T''[S_s^{1/2}(1) + S_t^{1/2}(1)]\}, \quad (50a)$$

$$S_{00}^{1/2} = \frac{1}{2}T'[S_s^{1/2}(1) + S_t^{1/2}(1)], \quad (50b)$$

$$S_{10}^{1/2} = -\frac{1}{2}\{T^s[S_s^{1/2}(1) - S_t^{1/2}(1)] + T''[S_s^{1/2}(1) + S_t^{1/2}(1)]\}, \quad (50c)$$

$$S_{11}^{1/2} = -S_{00}^{1/2}, \quad (50d)$$

$$S_{01}^{3/2} = -T''S_s^{3/2}(1), \quad (50e)$$

$$S_{11}^{3/2} = T'S_s^{3/2}(1) \quad (50f)$$

with ($n = s$ or t)

$$S_n^{1/2}(\alpha) = g_n(\vec{k}_\alpha) \tau_n \left(z - \frac{3p_\alpha^2}{4M} \right) \times [I_n^{1/2}(\vec{p}_\alpha, z) + I_{n_s}^{1/2}(\vec{p}_\alpha, z)], \quad (51)$$

$$S_s^{3/2}(\alpha) = g_s(\vec{k}_\alpha) \tau_s \left(z - \frac{3p_\alpha^2}{4M} \right) J_{ss}^{3/2}(\vec{p}_\alpha, z), \quad (52)$$

and

$$I_{nn'}^I(\vec{p}, z) = \int d^3p' \langle \vec{p} | X_{nn'}^I(z) | \vec{p}' \rangle \times \tau_n \left(z - \frac{3p'^2}{4M} \right) B_n^{0I}(z, \vec{p}). \quad (53)$$

Thus, the application of Eq. (35) to ${}^3\text{He}$ photodisintegration leads us to six possible amplitudes as delineated in Table I and expressible as

$$M_{S_{23}I_{23}}^I(z, \vec{p}, \vec{k}) = C_{S_{23}I_{23}}^I(\vec{p}, \vec{k}) + F_{S_{23}I_{23}}^I(z, \vec{p}, \vec{k}) + S_{S_{23}I_{23}}^I(z, \vec{p}, \vec{k}) \quad (54)$$

through Eqs. (44)–(53).

Once the amplitudes have been obtained numerically (see Appendixes A and B for the practical aspects of partial waves and numerical methods), the three-body differential cross section is obtained from

$$d\sigma = \frac{4\pi^2}{\hbar c} E_\gamma \sum_{S_{23}=0}^1 \left| \mathfrak{M}_{S_{23}}^{S_{23}} \left(\frac{3p^2}{4M} + \frac{k^2}{M}, \vec{p}, \vec{k} \right) \right|_{\text{pol. av.}}^2 \rho_f, \quad (55)$$

where E_γ is the photon energy and ρ_f is the density of final states. The form of $\mathfrak{M}_{S_{23}}^{S_{23}}$ depends on which nucleon is designated particle 1. For example,

TABLE II. Parameters for the separable N-N interactions.

Interaction	λ (fm $^{-3}$)	β (fm $^{-1}$)	a (fm)	r_0 (fm)	
I	V_t	0.391	1.418	5.397	1.747
	V_s	0.148	1.150	-21.25	2.74
II	V_t	0.3815	1.406	5.423	1.761
	V_s	0.1323	1.130	-17.0	2.84
III	V_t	0.3815	1.406	5.423	1.761
	V_s	0.1534	1.223	-7.823	2.794

if we wish to consider the reaction ${}^3\text{He}(\gamma, n)2p$, it is convenient to designate the neutron as particle 1, then

$$\mathfrak{N}_3^{S_{23}} = -\sqrt{\frac{2}{3}}M_{S_{23}^1}^{1/2} + \sqrt{\frac{1}{3}}M_{S_{23}^1}^{3/2}; \quad (56)$$

however, if the reaction is ${}^3\text{He}(\gamma, p)np$ or ${}^3\text{He}(\gamma, 2p)n$, it is convenient to choose one of the protons as particle 1, then

$$\mathfrak{N}_3^{S_{23}} = \frac{1}{\sqrt{2}}(M_{S_{23}^0}^{1/2} + \sqrt{\frac{1}{3}}M_{S_{23}^1}^{1/2} + \sqrt{\frac{2}{3}}M_{S_{23}^1}^{3/2}). \quad (57)$$

In the former case, we need only four of the six possible amplitudes, whereas all six are needed in the latter case.⁹

IV. RESULTS

In our calculations of the three-body photodisintegration we have used primarily two models: (1) Barbour and Phillips' ground-state I plus a final state from the potentials labeled I in our Table II; (2) our own model in which both the ground state and the final state are generated from the same N - N potentials labeled II in our Table II. The ground-state wave function is written as

$$\psi_0^S(\vec{k}, \vec{p}) = \psi^{(1)} + \psi^{(2)} + \psi^{(3)}, \quad (58)$$

where

$$\psi^{(1)} = N_3 \frac{g_t(k)u_t(p) + g_s(k)u_s(p)}{k^2 + \frac{3}{4}p^2 + K^2} \quad (59)$$

and $K^2 = ME_B$. Here $\psi^{(k)}$ refers to the (ij, k) per-

mutation of the three-body relative momentum variables $(\vec{k}_{ij}, \vec{p}_k)$. The form factors are of the standard Yamaguchi type

$$g_n(k) = (k^2 + \beta_n^2)^{-1}, \quad (60)$$

and the numerical spectator functions are parameterized by the analytic form

$$u_n(p) = C_n / (1 + \bar{\alpha}_n p^2 + \bar{\beta}_n p^4 + \bar{\gamma}_n p^6). \quad (61)$$

The parameters of the spectator functions are listed in Table III along with the normalization constant N_3 . Because s -wave models of the type described here are known to overbind (due in part to an absence of the tensor force in the triplet state), we have altered the triplet strength λ_t for our model to a value of 0.354 in order to ensure that our ${}^3\text{He}$ ground state has the correct binding energy of 7.72 MeV. A more complete discussion of the bound states can be found in Ref. 1 along with an analysis of their asymptotic properties.

We first checked to assure that our calculations were consistent with those of Barbour and Phillips. The slight differences in the singlet parameters (they used $a_s = -20.34$ fm and $r_s = 2.7$ fm) between the two calculations are of essentially no consequence. However, we should emphasize that we have restricted the ground state to the symmetric S component, so that a direct comparison of our figures with theirs is not possible in most cases.

We then proceeded to calculate the cross section for both ${}^3\text{He}(\gamma, n)2p$ and ${}^3\text{He}(\gamma, p)np$ using the latter model discussed above. In Fig. 2 we break down the cross section for $T = \frac{3}{2}$ and $T = \frac{1}{2}$ into Born, Born plus first rescattering, and full calculation. The short dashed curve is the plane-wave Born result for either isospin component of the cross section. The long dashed curves are the plane-wave Born plus first-rescattering results; i.e., the first two diagrams in the photodisintegration amplitude sum shown in Fig. 1. The upper curve is for the $T = \frac{3}{2}$ component and the lower curve is for the $T = \frac{1}{2}$ component. Note that this first rescattering greatly enhances the $T = \frac{3}{2}$ cross section while the $T = \frac{1}{2}$ cross section is lowered by about a factor of 2. The solid curves describe the full calculation for both components, the $T = \frac{3}{2}$ curve again being the upper one. For the full calculation, the $T = \frac{3}{2}$

TABLE III. Ground-state wave function parameters.

Wave function	B_3 (MeV)	N_3 (fm $^{-1}$)	C	$\bar{\alpha}$	$\bar{\beta}$	$\bar{\gamma}$	
I Barbour-Phillips	7.71	0.372	1.0	6.15	2.89	0.353	(triplet)
			0.310	4.31	1.17	0.0821	(singlet)
II Adjusted triplet ($\lambda_t = 0.354$)	7.72	0.307	1.000	4.93	1.92	0.133	(triplet)
			0.335	3.38	0.913	0.0907	(singlet)

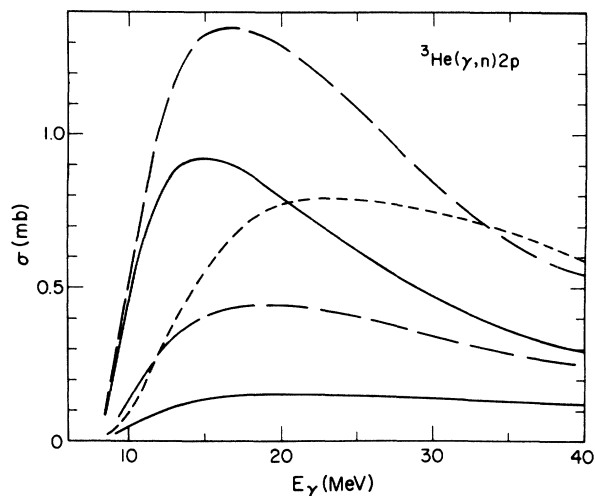


FIG. 2. A decomposition of the $T=\frac{3}{2}$ and $T=\frac{1}{2}$ components of the total ${}^3\text{He}(\gamma, n)2p$ cross section. The (---) curve is the plane-wave Born result for either isospin. The (—) curve is the first-rescattering result; the upper curve is $T=\frac{3}{2}$, the lower curve is $T=\frac{1}{2}$. The (—) curve is the complete result; the upper curve is again $T=\frac{3}{2}$, the lower curve is $T=\frac{1}{2}$. The calculation is for our model described in Sec. IV.

result is reduced from the first-rescattering curve to a peak value approaching the plane-wave Born result; however, the final-state rescattering has moved the peak from about 25 MeV photon energy to below 15 MeV, and the cross section is strongly enhanced below 20 MeV while suppressed above 20 MeV compared to the plane-wave Born result. The $T=\frac{1}{2}$ component is suppressed even further from the plane-wave Born result; the strength of this component of the three-body channel is lost

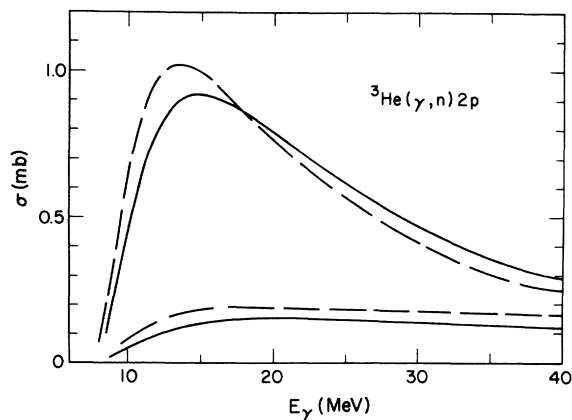


FIG. 3. Comparison of the $T=\frac{3}{2}$ (upper two curves) and the $T=\frac{1}{2}$ (lower two curves) total cross sections for the Barbour-Phillips model (---) and our model (—).

to the two-body breakup channel. (See Ref. 1 for a discussion of the mechanism for this enhancement of the two-body channel.) We note that a second-rescattering approximation to the $T=\frac{3}{2}$ component of the cross section is sufficient to come within 10% of the final result (the upper solid curve); by second rescattering, we mean substitution of the driving term (Born term) of the integral equation in Fig. 1 for the off-shell amplitude X_{mn} in the third term of the sum for M_3 in Fig. 1. Such is not the case for the $T=\frac{1}{2}$ component; in the $T=\frac{1}{2}$ case the series converges slowly and the complete solution of the integral equation is required.

In Fig. 3 we compare our complete solutions for the two models discussed. The dashed curves are for the Barbour and Phillips model; the solid curves are for our model. Below 20 MeV both our $T=\frac{3}{2}$ (upper curve) and $T=\frac{1}{2}$ (lower curve) results are below the Barbour-Phillips result. As in the two-body photodisintegration reaction,⁽¹⁾ this difference is due to the double-pole parametrization of the ground-state spectator. Such a parametrization fitted to the rms radius of ${}^3\text{He}$ appears to overemphasize the asymptotic region of the wave function; i.e., it leads to too large a normalization of the tail of the wave function which is emphasized by the $(\hat{\epsilon} \cdot \vec{r})$ long wavelength limit of the electric dipole operator. Above 20 MeV the differences in the $T=\frac{3}{2}$ and $T=\frac{1}{2}$ isospin components of the cross sections compensate, so that the result for the complete cross section is essentially the same for the two models. Note that the lower cross section in the $T=\frac{1}{2}$ channel at higher photon energies means that our two-body cross section will be larger than the Barbour-Phillips prediction

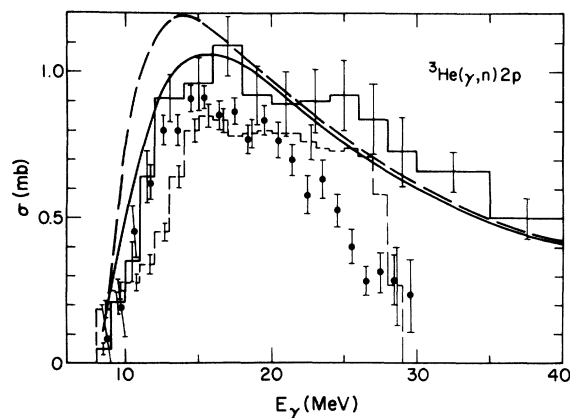


FIG. 4. Comparison of the total cross section for our model (—) and the Barbour-Phillips model (---) with the data of the Ref. 3 (broken histogram), Ref. 4 (—), and Ref. 5 (solid histogram).

at these energies as was indeed found to be the case in Ref. 1.

In Fig. 4 we compare the cross sections for the two models (symmetric S state only) and the available data. Our model result peaks some 15% below the Barbour-Phillips result—a feature that was also true in the two-body photodisintegration reaction.¹ Our calculation peaks about 10% higher than the data would appear to indicate; such a discrepancy is likely due to our neglect of the tensor force although a complete treatment of the S' state and Coulomb effects should improve the fit also. Note that we confirm the strong enhancement of the cross section at low energies (where the cross section is dominated by $T = \frac{3}{2}$) found by Barbour and Phillips but absent in the work of Fabre and Levinger. Without this strong rescattering enhancement, the fit to the data at low photon energies would be very poor, since the $T = \frac{3}{2}$ plane-wave Born result very much underestimates the cross section below 15 MeV.

In addition to the total cross section, we have calculated both the neutron and proton energy spectra from ${}^3\text{He}$. In Figs. 5 and 6 we compare our results with the data of Gorbunov⁵ in the photon energy region 12–16 MeV. In Fig. 5 we compare the neutron energy spectra. The neutron is the odd particle, so that one sees the very strong p - p final-state interaction near $E_n/E_{\text{max}} \approx 1.0$. Note also the region around $E_n/E_{\text{max}} \approx 0.2$; Barbour and Phillips have previously pointed out the enhancement of the spectra in this region (due to n - p rescattering). Because Gorbunov does not quote absolute normalization we have conveniently normalized our two curves for $E_\gamma = 12.5$ and 15.5 MeV; however, the relative normalization of the two curves is correct. The fact that the peak in the data near $E_n/E_{\text{max}} = 1.0$ is shifted relative to both curves is probably a reflection of our neglect of

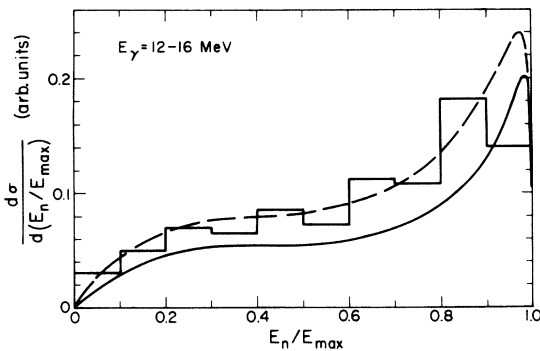


FIG. 5. Comparison of the shape of the experimental spectrum from Ref. 5 with our theoretical spectra at $E_\gamma = 12.5$ MeV (---) and $E_\gamma = 15.5$ MeV (—) for the reaction ${}^3\text{He}(\gamma, n)2p$.

the Coulomb interaction.

In Fig. 6 we compare our spectra from the ${}^3\text{He}(\gamma, p)n2p$ reaction with the data of Gorbunov.⁵ The qualitative features are again correct. The n - p interaction enhancement near $E_p/E_{\text{max}} \approx 1.0$ is much weaker than that of the p - p in the previous spectrum. The largest enhancement occurs near $E_p/E_{\text{max}} \approx 0.2$ where the p - p rescattering is strong. Again the relative normalization of our curves for photon energies of 12.5 and 15.5 MeV is correct, but there is no absolute normalization for the curves or the data.

As pointed out above, we have neglected the Coulomb interaction between the two protons. In order to investigate qualitatively the effect of including the Coulomb repulsion, we have used in the final state the singlet potential labeled III in Table II. By so doing we approximate the effect of the long-range electromagnetic interaction of the strong p - p interaction as a weakening of the short-range attractive N - N potential. Such an approximation is clearly not theoretically correct in a proper treatment of the scattering problem; however, it will permit us to examine qualitative features, and the bound state wave function does cut off the matrix element integral short of the asymptotic region for the scattering state. Since we have seen above that strong final-state interactions enhance the $T = \frac{3}{2}$ and suppress the $T = \frac{1}{2}$ components of the total cross section below 20 MeV, the use of a slightly weaker singlet potential such as III in Table II reduces both of these effects, and the compensating changes leave the total cross section essentially unchanged below $E_\gamma = 20$ MeV. Similarly the cross section is increased slightly (<5%) above 20 MeV. The effect is, of course, much larger in the proton and neutron spectra.

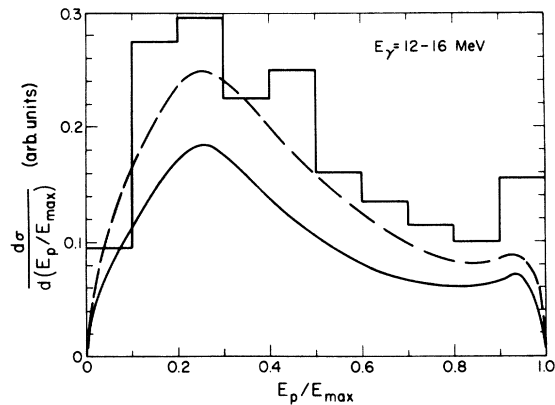


FIG. 6. Comparison of the shape of the experimental spectrum from Ref. 5 with our theoretical spectra at $E_\gamma = 12.5$ MeV (---) and $E_\gamma = 15.5$ MeV (—) for the reaction ${}^3\text{He}(\gamma, p)n2p$.

The p - p interaction is weakened, so that in the ${}^3\text{He}(\gamma, n)2p$ spectra, for example, the sharp peak near $E_n/E_{\text{max}} \approx 1.0$ is broadened and reduced in magnitude. This is displayed explicitly in Fig. 7, where we show the curves from Fig. 5 and the corresponding curves in the region of the p - p final-state interaction calculated with the Coulomb weakened singlet potential III from Table II. (Because the n - p singlet interaction is actually stronger than the singlet potential II of Table III, we have not shown the spectra for potential III in the region where the n - p final-state interaction dominates.) It is clear from the figure that including Coulomb effects, even in this approximation, moves the calculation in the right direction: the p - p peak is lowered, broadened, and shifted to lower energy, although the shift is not enough to agree with the data.

V. CONCLUSIONS

In summary, the primary conclusions to be drawn from this work are as follows: (1) The peak value of the total cross section is about 1 mb, in reasonable agreement with the data. (2) Differences between our theoretical results and the data arise from neglect of the tensor nature of the triplet force, the S' component of the ${}^3\text{He}$ wave function, and the pure Coulomb repulsion in the p - p interaction. (3) Our total cross section is some 15% below that of the Barbour-Phillips model in the region of the peak, the difference being due primarily to the double-pole analytic form assumed for the ground-state spectator function in their model. (4) For the $T = \frac{3}{2}$ isospin channel the second-rescattering approximation comes within 10% of the complete answer, a fact that may be useful

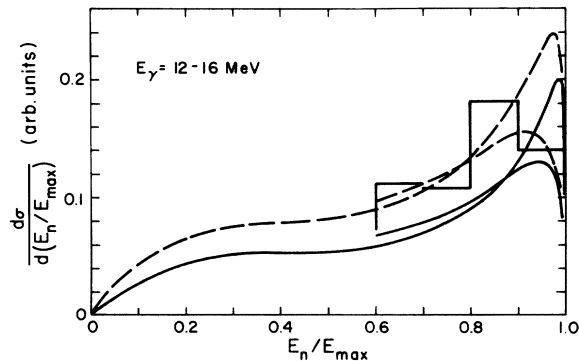


FIG. 7. Comparison of the experimental spectrum from Ref. 5 and our theoretical spectra at 12.5 MeV (—) and 15.5 MeV (—) without Coulomb effects as shown in Fig. 5 with theoretical spectra including some Coulomb effects (the partial curves) in the approximation discussed in Sec. IV.

for reactions such as ${}^3\text{H}(\pi^-, \gamma)3n$ where there is only a $T = \frac{3}{2}$ component in the final state. (5) Almost all of the $T = \frac{1}{2}$ cross section is lost to the ${}^3\text{H}(\gamma, d)p$ channel; the mechanism for this is discussed in detail in Ref. 1. (6) The shapes of the experimental ${}^3\text{He}(\gamma, n)2p$ and ${}^3\text{He}(\gamma, p)np$ spectra are reproduced qualitatively showing the effects of the strong final-state p - p interaction. (7) The position and shape of the main peak in the ${}^3\text{He}(\gamma, n)2p$ spectra were improved by inclusion of Coulomb effects on the p - p strong interaction in the final state in a very approximate manner, but a substantial quantitative discrepancy remains.

ACKNOWLEDGMENTS

One of the authors (DRL) wishes to thank the George Washington University Committee on Research for a summer research grant from National Science Foundation Institute Grant No. GU3287. A part of the computer time for this work was provided by the George Washington University computer center.

APPENDIX A: PARTIAL WAVES

The practical problem of computing the amplitude $\langle \vec{p} | X_{nn'}^I(z) | \vec{p} \rangle$ for Eq. (53) is handled by partial-wave decomposition. This is done in the same manner as described in Sec. III of Ref. 1. The only difference is that, in addition to the isospin- $\frac{1}{2}$ equations given there, we now have to consider the isospin- $\frac{3}{2}$ continuum equation. There is a single equation of the form given by Eq. (48) (Ref. 1) with all subscripts being singlet. The inhomogeneous term is

$$Z_{ss}^{3/2J}(p, p'; z) = -\frac{1}{2} \int_{-1}^1 dx \frac{P_J(x) g_s(q^2) g_s(q'^2)}{p^2 + p'^2 + pp'x - Mz}, \quad (\text{A1})$$

where $P_J(x)$ is the Legendre function for angular momentum J and

$$q^2 = \frac{1}{4} p^2 + p'^2 + pp'x, \quad (\text{A2})$$

$$q'^2 = p^2 + \frac{1}{4} p'^2 + pp'x. \quad (\text{A3})$$

Then Eq. (53) can be written as

$$I_{nn'}^I(\vec{p}, z) = 4\pi \hat{e} \cdot \hat{p} \int_0^\infty p'^2 dp' X_{nn'}^I(p, p'; z) \times \tau_{nn'} \left(z - \frac{3p'^2}{4m} \right) \mathcal{R}_n^{0I}(z, p') \quad (\text{A4})$$

with $E_n^{0I}(z, \vec{p}) = \hat{e} \cdot \hat{p} \mathcal{R}_n^{0I}(z, p)$.

APPENDIX B: NUMERICAL METHODS

There are two situations for which it is worthwhile to explain our numerical methods.

The first situation involves the off-shell Born amplitudes when evaluated on shell as in the first-rescattering terms. Take, as an example, the following

$$(z = 3p^2/4M + k^2/M + i\eta) :$$

$$B_s^{\text{os}/2}(z, \vec{p}) = \frac{eM}{\sqrt{3}} \int d^3k' \frac{g_s(k') [\hat{\epsilon} \cdot \vec{p}_{op} \psi_0^s(\vec{k}, \vec{p})]}{k'^2 - k^2 - i\eta}. \quad (\text{B1})$$

Such integrals are rewritten as the sum of a pole contribution plus a principal-value integral. The principal-value integral is then evaluated by standard numerical methods, after utilizing the fact that

$$P \int_0^\infty \frac{dk'}{k'^2 - k^2} \equiv 0 \quad (\text{B2})$$

to subtract

$$P \int_0^\infty \frac{dk'}{k'^2 - k^2} k^2 g_s(k) \left[\int d\Omega_{k'} \hat{\epsilon} \cdot \vec{p}_{op} \psi_0^s(k\hat{k}', \vec{p}) \right] = 0. \quad (\text{B3})$$

The second situation concerns evaluation of the integrals in Eq. (53), or equivalently, Eq. (A2). After studying the singularities of the integrand, which includes the problem of solving for $X_{nm}^{I1}(p, p'; z)$, it becomes apparent that rotating the p' integration path into the fourth quadrant would be an appropriate method, i.e., $p' \rightarrow p'e^{-i\phi}$. This requires consideration of two cases:

$$\text{Case I: } 0 \leq p \leq \sqrt{Mz}, \quad (\text{B4})$$

$$\text{Case II: } \sqrt{Mz} < p \leq 2\sqrt{Mz}/3. \quad (\text{B5})$$

Case I

Investigation of the integral equation for $X_{nm}^{I1}(p, p'; z)$ indicates that the only constraint from this source is

$$\tan\phi < \min\left(\frac{2\beta_n}{p}, \frac{\beta_n}{p}\right). \quad (\text{B6})$$

$\tau_{nr}(z - 3p'^2/4M)$ and $B_n^{\text{os}/2}(z, \vec{p}')$ introduce no constraints provided $B_n^{\text{os}/2}(z, \vec{p}')$ is handled as $B_n(z, \vec{p}')$

$$\begin{aligned} & \int_0^\infty p'^2 dp' X_{nm}^{I1}(p, p'; z) \tau_{nr}\left(z - \frac{3p'^2}{4M}\right) \mathcal{B}_n^{\text{os}/2}(z, p') \\ &= \frac{2\pi i}{p} c_{nm}^I g_n \left(\left(Mz - \frac{3p^2}{4} \right)^{1/2} \right) \int_0^{p_n} p' dp' g_{nr} \left(\left(Mz - \frac{3p'^2}{4} \right)^{1/2} \right) P_1 \left(\frac{Mz - p^2 - p'^2}{pp'} \right) \tau_{nr}\left(z - \frac{3p'^2}{4M}\right) \mathcal{B}_n^{\text{os}/2}(z, p') \\ &+ \left[\int_0^{p_B e^{i\phi}} \left(\text{second sheet} \right) + \int_{p_B e^{i\phi}}^\infty \left(\text{first sheet} \right) \right] p'^2 dp' e^{-i3\phi} X_{nm}^{I1}(p, p' e^{-i\phi}; z) \tau_{nr}\left(z - \frac{3p'^2}{4M} e^{-i2\phi}\right) \mathcal{B}_n^{\text{os}/2}(z, p' e^{-i\phi}), \quad (\text{B7}) \end{aligned}$$

where c_{nm}^I are the coefficients from Z_{nm}^{I1} , defined in Ref. 1:

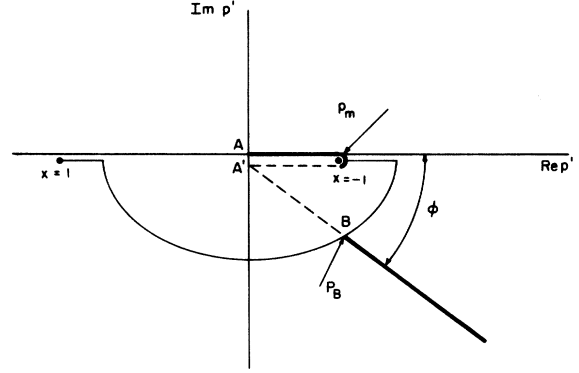


FIG. 8. Integration contour for the integral in Eq. (53) when $\sqrt{Mz} < p \leq 2\sqrt{Mz}/3$. The values of p_m and p_B are given by $p_m = \frac{1}{2}p - (Mz - 3p^2/4)^{1/2}$ and $p_B = e^{-i\phi}(p^2 - Mz)^{1/2}$.

was in Ref. 1. This requires breaking $B_n^{\text{os}/2}(z, \vec{p}')$ into two parts: that which requires only a k integration and that which requires both a k integration and an angular integration. When $p' \rightarrow p'e^{-i\phi}$, the part which does not require an angular integration is computed by rotating $k \rightarrow ke^{-i\phi/4}$, while the part with an angular integration is done with k rotated the same as p' , i.e., $k \rightarrow ke^{-i\phi}$. (Note: In the second part, the variables must be changed to make the spectator function argument simply \vec{k} .) The rotation angle ϕ is chosen to be half its maximum allowed value given by Eq. (B6).

Case II

In order to rotate $p' \rightarrow p'e^{-i\phi}$ for this range of p , we must account for the cut structure of $X_{nm}^{I1}(p, p'; z)$, or equivalently, of $Z_{nm}^{I1}(p, p'; z)$ [see the partial-wave form of Eq. (37)]. The cut of interest arises from the energy denominator $p'^2 + pp'x + p^2 - z = 0$ of $Z_{nm}^{I1}(p, p'; z)$ and we display it in Fig. 8.¹⁰ We also show in this figure how the contour is distorted around the cut (taking into account that z has a small positive imaginary part, i.e., $z + i\eta$). It is evident from Fig. 8 that the integral in Eq. (53) or Eq. (A2) will break into the following pieces:

$$\begin{bmatrix} c_{tt}^{1/2} & c_{ts}^{1/2} \\ c_{st}^{1/2} & c_{ss}^{1/2} \end{bmatrix} = \begin{bmatrix} \frac{1}{4} & -\frac{3}{4} \\ -\frac{3}{4} & \frac{1}{4} \end{bmatrix}; \quad c_{ss}^{3/2} = -\frac{1}{2}.$$

The first term comes from the integration $A \rightarrow p_m \rightarrow A'$ expressed as an integral from 0 to p_m over the discontinuity across the cut. This discontinuity is calculated utilizing the fact that the discontinuity of $X_{nn'}^{I1}(p, p'; z)$ across the cut is equal to the discontinuity of $Z_{nn'}^{I1}(p, p'; z)$ across the cut. The second term must be done carefully, since from A' to B $X_{nn'}^{I1}(p, p'e^{-i\phi}; z)$ is to be evaluated on the second sheet (dashed line). This requires that we solve the following modified equations for $X_{nn'}^{I1}(p, p'e^{-i\phi}; z)$:

$$0 \leq p' \leq p_B e^{i\phi} = (p^2 - Mz)^{1/2} \quad (\text{second sheet}):$$

$$X_{nn'}^{I1}(p, p'e^{-i\phi}; z) = Z_{nn'}^{I1}(p, p'e^{-i\phi}; z)_{\text{second sheet}}$$

$$\begin{aligned} & + \frac{8\pi^2 i}{p} g_n \left(\left(Mz - \frac{3p^2}{4} \right)^{1/2} \right) \sum_{n''=s}^t c_{nn''}^I \int_0^{p_m} p'' dp'' Z_{n''n''}^I(p'e^{-i\phi}, p''; z) \\ & \quad \times \tau_{n''} \left(z - \frac{3p''^2}{4M} \right) g_{n''} \left(\left(Mz - \frac{3p''^2}{4} \right)^{1/2} \right) P_1 \left(\frac{Mz - p^2 - p''^2}{pp''} \right) \\ & + 4\pi \sum_{n''=s}^t \left[\int_0^{p_B e^{i\phi}} \left(\text{second sheet} \right) + \int_{p_B e^{i\phi}}^\infty \left(\text{first sheet} \right) \right] p''^2 dp'' e^{-i3\phi} Z_{n''n''}^I(p'e^{-i\phi}, p'' e^{-i\phi}; z) \\ & \quad \times \tau_{n''} \left(z - \frac{3p''^2}{4M} e^{-i2\phi} \right) X_{nn''}^I(p, p'' e^{-i\phi}; z) \end{aligned} \quad (\text{B8})$$

$$p_B e^{i\phi} \leq p' < \infty \quad (\text{first sheet}):$$

$$\begin{aligned} X_{nn'}^{I1}(p, p'e^{-i\phi}; z) & = Z_{nn'}^{I1}(p, p'e^{-i\phi}; z)_{\text{first sheet}} \\ & + [\text{same as Eq. (B8)}]. \end{aligned} \quad (\text{B9})$$

The only other stipulation entering the calculations for this case is from $B_{n'}^{0I}(z, \vec{p}')$ for $0 \leq p' \leq p_m$. The angle-independent k integral is still rotated 45° into the fourth quadrant, but the rotation for

the k integration which also includes an angular integral is chosen as

$$\phi = \frac{1}{2} \tan^{-1} \left[\min \left(\frac{2(K^2 + \frac{3}{4}p'^2)^{1/2}}{p'}, \frac{2\beta_{n'}}{p'}, \frac{\beta}{p} \right) \right], \quad (\text{B10})$$

where the unsubscripted β is the smallest β appearing in the $g_n(k)$ of the ground-state wave function. For all other regions, $B_{n'}^{0I}(z, \vec{p}')$ is handled as in case I.

[†]Work done under the auspices of the U.S. Energy Research and Development Association.

¹B. F. Gibson and D. R. Lehman, Phys. Rev. C **11**, 29 (1975).

²V. N. Fetisov, A. N. Gorbunov, and A. T. Varfalomeev, Nucl. Phys. **71**, 305 (1965).

³H. M. Gerstenberg and J. S. O'Connell, Phys. Rev. **144**, 834 (1966).

⁴B. L. Berman, S. C. Fultz, and P. F. Yergin, Phys. Rev. C **10**, 2221 (1974).

⁵A. N. Gorbunov, in *Photonuclear and Photomesic Processes*, Proceedings of the P. N. Lebedev Physics Institute, 1974 (Nauka, Moscow, 1974), Vol. **71**, p. 1.

⁶I. M. Barbour and A. C. Phillips, Phys. Rev. C **1**, 165

(1970).

⁷M. Fabre de la Ripelle and J. S. Levinger, Nuovo Cimento **25A**, 555 (1975).

⁸If the reader compares Eqs. (9), (12), (14), (15), and (20) of this section with Eqs. (9), (12), (17), (21), and (23), respectively, of Ref. 1, he will note that the equations of this paper can be obtained from those of Ref. 1 by extending the range of the index α to include the value zero.

⁹Of course, computation of the total cross section with either Eq. (56) or (57) yields the same result. Also, in the total cross section, the isospin-1/2 and isospin -3/2 amplitudes do not interfere.

¹⁰R. Aaron and R. D. Amado, Phys. Rev. **150**, 857 (1966).